Hindawi
International Journal of Antennas and Propagation
Volume 2017, Article ID 3424536, 6 pages
https://doi.org/10.1155/2017/3424536

Research Article

Tolerance Analysis of Antenna Array Pattern and Array Synthesis in the Presence of Excitation Errors

Ying Zhang, DanNi Zhao, Qiong Wang, ZhengBin Long, and Xiaofeng Shen

College of Electronic Engineering, University of Electronic Science and Technology of China, Chengdu, Sichuan 611731, China

Correspondence should be addressed to Xiaofeng Shen; sxf.uestc@163.com

Received 28 December 2016; Accepted 16 March 2017; Published 11 July 2017

Academic Editor: Yumao Wu

This paper analyzes array pattern tolerance against excitation errors. The nonprobabilistic interval analysis algorithm is used for tolerance analysis of the nonideal uniform linear array in this work. Toward this purpose, corresponding interval models of the power pattern functions are established, respectively, with the consideration of the amplitude errors, phase errors, or both simultaneously, in antenna arrays. The tolerance for the amplitude-phase error of the main function parameters including the beamwidth, sidelobe level, and the directivity is simulated by computer according to the indicators and the actual requirements. Accordingly, the worst admissible performance of an array can be evaluated, which may provide theoretical reference for optimal antenna array design. As for the problem of array synthesis in the presence of various array errors, interval analysis-convex programming (IA-CP) is presented. Simulation results show that the proposed IA-CP based synthesis technique is robust for the amplitude and phase errors.

1. Introduction

Antenna arrays are widely used for their flexibility and reliability in wireless data transmission. For array design, an important performance indicator is the radiation pattern. In real applications, excitation errors including amplitude error and phase error widely existed due to manufacturing errors. Excitation errors affect radiation pattern of arrays, which usually deteriorates performance of the designed arrays. Therefore, the effect of excitation errors on array radiation pattern should be analyzed for robust array design [1].

Traditional error analysis strategies are generally based on the statistical theory. For instance, under the assumption that the excitation errors are normally distributed, Ruze proposed analyzing the association between the radiation pattern and the random excitation errors [2]. In [3], Hsiao obtained the statistical regularities of sidelobes distributed in different regions by studying the impacts of stochastic independence and corresponding amplitude-phase errors on the sidelobe level. However, these statistical methods cannot be applied into engineering design directly as the distribution of amplitude and phase errors may be unknown.

To resolve this issue, a novel approach based on interval arithmetic (IA) was proposed in [4]. IA was originally introduced for the computation of the rounding errors when using numerical resolution strategies [5, 6]. It was then extended to deal with nonlinear equations [7] as well as optimization problems [8, 9]. Recently, this method has been successfully applied to compute the bounds of the radiation pattern when array excitation errors exist [4, 10–13]. Existing IA-based analysis methods showed satisfactory results. Nevertheless, there has been no literation considering the case where excitation amplitude and phase errors simultaneously exist.

In this paper, the excitation amplitude and phase errors are considered simultaneously to achieve the upper and lower bounds of array radiation patterns. Tolerance of array radiation pattern is analyzed by interval arithmetic (IA). Since excitation phase error has different influence on the real and imaginary parts of the radiation pattern, the optimal bounds are hard to achieve. Instead, a relaxed version bound is presented. Accordingly, the worst admissible performance of an array can be evaluated, which may provide theoretical reference for optimal antenna array design. As for the problem of array synthesis in the presence of various array errors,

a method based on interval analysis-convex programming (IA-CP) is given. Simulation results show that the IA-CP-based synthesis technique is not only robust for the amplitude and phase errors, but also suitable for large arrays.

2. Radiation Pattern Tolerance Analysis in the Presence of Excitation Amplitude and Phase Errors

2.1. Analysis Based on Interval Arithmetic. Consider a uniform linear array with N elements. Assume the real excitation amplitude and phase on the nth element are denoted by α_n and φ_n, respectively. The array factor interval is given by

$$\mathrm{AF}^I(\theta) = \sum_{n=0}^{N-1} \mathrm{AF}_n^I(\theta) = \sum_{n=0}^{N-1} \alpha_n^I e^{j\Theta_n^I(\theta)}, \tag{1}$$

where $\alpha_n^I = [\alpha_n^L, \alpha_n^U]$ denotes the amplitude interval. $\Theta_n^I(\theta) = nkd\sin\theta + \varphi_n^I$, where $\varphi_n^I = [\varphi_n^L, \varphi_n^U]$ denotes the phase interval. $\theta \in [-\pi/2, \pi/2]$ is the angular direction measured from boresight, $j = \sqrt{-1}$ is the unit complex number, d denotes element space, and $k = 2\pi/\lambda$ is the wavenumber.

The interval of power pattern is given by

$$P^I(\theta) = \left[\mathrm{AF}_{\Re}^I(\theta)\right]^2 + \left[\mathrm{AF}_{\Im}^I(\theta)\right]^2, \tag{2}$$

where $\mathrm{AF}_{\Re}^I(\theta)$ and $\mathrm{AF}_{\Im}^I(\theta)$ denote the real and imaginary part of $\mathrm{AF}^I(\theta)$, respectively.

In the presence of amplitude and phase error, it is difficult to determine the upper and lower bound of (2), since the real and imaginary parts of power pattern are coupled with phase. Use the fact that

$$\begin{aligned} &\max\left\{\mathrm{AF}_{\Re}^2(\theta) + \mathrm{AF}_{\Im}^2(\theta)\right\} \\ &\quad \le \max\left\{\mathrm{AF}_{\Re}^2(\theta)\right\} + \max\left\{\mathrm{AF}_{\Im}^2(\theta)\right\}, \\ &\min\left\{\mathrm{AF}_{\Re}^2(\theta) + \mathrm{AF}_{\Im}^2(\theta)\right\} \\ &\quad \ge \min\left\{\mathrm{AF}_{\Re}^2(\theta)\right\} + \min\left\{\mathrm{AF}_{\Im}^2(\theta)\right\}. \end{aligned} \tag{3}$$

A relaxed version of the upper and lower bound of power pattern is proposed as

$$P^U(\theta) = \left[\mathrm{AF}_{\Re}^U(\theta)\right]^2 + \left[\mathrm{AF}_{\Im}^U(\theta)\right]^2, \tag{4a}$$

$$P^L(\theta) = \left[\mathrm{AF}_{\Re}^L(\theta)\right]^2 + \left[\mathrm{AF}_{\Im}^L(\theta)\right]^2. \tag{4b}$$

Then, similar to [4], the upper and lower bounds can be expressed by the midpoint and the interval width of $\mathrm{AF}_{\Re}^I(\theta)$ and $\mathrm{AF}_{\Im}^I(\theta)$:

$$P^U(\theta) = \left(\left|\mu\left\{\mathrm{AF}_{\Re}^I(\theta)\right\}\right| + \frac{\omega\left\{\mathrm{AF}_{\Re}^I(\theta)\right\}}{2}\right)^2 + \left(\left|\mu\left\{\mathrm{AF}_{\Im}^I(\theta)\right\}\right| + \frac{\omega\left\{\mathrm{AF}_{\Im}^I(\theta)\right\}}{2}\right)^2, \tag{5a}$$

$$P^L(\theta) = \begin{cases} \left(\left|\mu\left\{\mathrm{AF}_{\Re}^I(\theta)\right\}\right| - \dfrac{\omega\left\{\mathrm{AF}_{\Re}^I(\theta)\right\}}{2}\right)^2, & 0 \notin \mathrm{AF}_{\Re}^I,\ 0 \in \mathrm{AF}_{\Im}^I \\ \left(\left|\mu\left\{\mathrm{AF}_{\Im}^I(\theta)\right\}\right| - \dfrac{\omega\left\{\mathrm{AF}_{\Im}^I(\theta)\right\}}{2}\right)^2, & 0 \in \mathrm{AF}_{\Re}^I,\ 0 \notin \mathrm{AF}_{\Im}^I \\ \left(\left|\mu\left\{\mathrm{AF}_{\Re}^I(\theta)\right\}\right| - \dfrac{\omega\left\{\mathrm{AF}_{\Re}^I(\theta)\right\}}{2}\right)^2 + \left(\left|\mu\left\{\mathrm{AF}_{\Im}^I(\theta)\right\}\right| - \dfrac{\omega\left\{\mathrm{AF}_{\Im}^I(\theta)\right\}}{2}\right)^2, & 0 \notin \mathrm{AF}_{\Re}^I,\ 0 \notin \mathrm{AF}_{\Im}^I \\ 0, & \text{otherwise,} \end{cases} \tag{5b}$$

where $\mu\{\mathrm{AF}_{\Re}^I(\theta)\} = \sum_{n=0}^{N-1}\mu\{\mathrm{AF}_{n,\Re}^I(\theta)\}$, $\omega\{\mathrm{AF}_{\Re}^I(\theta)\} = \sum_{n=0}^{N-1}\omega\{\mathrm{AF}_{n,\Re}^I(\theta)\}$, $\mu\{\mathrm{AF}_{\Im}^I(\theta)\} = \sum_{n=0}^{N-1}\mu\{\mathrm{AF}_{n,\Im}^I(\theta)\}$, and $\omega\{\mathrm{AF}_{\Im}^I(\theta)\} = \sum_{n=0}^{N-1}\omega\{\mathrm{AF}_{n,\Im}^I(\theta)\}$.

The midpoint and the interval width of $\mathrm{AF}_{n,\Re}^I(\theta)$ and $\mathrm{AF}_{n,\Im}^I(\theta)$ are given by

$$\begin{aligned} \mu\left\{\mathrm{AF}_{n,\Re}^I(\theta)\right\} &= \frac{1}{2}\left[\mathrm{AF}_{n,\Re}^L(\theta) + \mathrm{AF}_{n,\Re}^U(\theta)\right], \\ \mu\left\{\mathrm{AF}_{n,\Im}^I(\theta)\right\} &= \frac{1}{2}\left[\mathrm{AF}_{n,\Im}^L(\theta) + \mathrm{AF}_{n,\Im}^U(\theta)\right], \end{aligned} \tag{6a}$$

$$\begin{aligned} \omega\left\{\mathrm{AF}_{n,\Re}^I(\theta)\right\} &= \mathrm{AF}_{n,\Re}^U(\theta) - \mathrm{AF}_{n,\Re}^L(\theta), \\ \omega\left\{\mathrm{AF}_{n,\Im}^I(\theta)\right\} &= \mathrm{AF}_{n,\Im}^U(\theta) - \mathrm{AF}_{n,\Im}^L(\theta). \end{aligned} \tag{6b}$$

Based on the rules of interval algorithm, $\mathrm{AF}_{n,\Re}^I(\theta)$ and $\mathrm{AF}_{n,\Im}^I(\theta)$ can be computed as

$$\begin{aligned} \mathrm{AF}_{n,\Re}^U(\theta) &= \begin{cases} A_n^L\cos^U\left(\Theta_n^I\right), & \cos^U\left(\Theta_n^I\right) < 0, \\ A_n^U\cos^U\left(\Theta_n^I\right), & \text{otherwise} \end{cases} \\ \mathrm{AF}_{\mathrm{n},\Re}^L(\theta) &= \begin{cases} A_n^L\cos^L\left(\Theta_n^I\right), & \cos^L\left(\Theta_n^I\right) > 0, \\ A_n^U\cos^L\left(\Theta_n^I\right), & \text{otherwise.} \end{cases} \end{aligned} \tag{7a}$$

$$\begin{aligned} \mathrm{AF}_{n,\Im}^U(\theta) &= \begin{cases} A_n^L\sin^U\left(\Theta_n^I\right), & \sin^U\left(\Theta_n^I\right) < 0, \\ A_n^U\sin^U\left(\Theta_n^I\right), & \text{otherwise} \end{cases} \\ \mathrm{AF}_{n,\Im}^L(\theta) &= \begin{cases} A_n^L\sin^L\left(\Theta_n^I\right), & \sin^L\left(\Theta_n^I\right) > 0, \\ A_n^U\sin^L\left(\Theta_n^I\right), & \text{otherwise.} \end{cases} \end{aligned} \tag{7b}$$

The lower and upper bounds of $\sin(\Theta_n^I)$ and $\cos(\Theta_n^I)$ are given by

$$\cos\left(\Theta_n^I(\theta)\right) = \begin{cases} \left[\cos\left(\Theta_n^L(\theta)\right), \cos\left(\Theta_n^U(\theta)\right)\right], & \dfrac{\partial\cos\left(\Theta_n^I\right)}{\partial\Theta_n^I} > 0, \\ \left[\cos\left(\Theta_n^U(\theta)\right), \cos\left(\Theta_n^L(\theta)\right)\right], & \dfrac{\partial\cos\left(\Theta_n^I\right)}{\partial\Theta_n^I} < 0, \\ \left[\min\left\{\cos\left(\Theta_n^L(\theta)\right), \cos\left(\Theta_n^U(\theta)\right)\right\}, 1\right], & 2i\pi \in \Theta_n^I, \\ \left[-1, \max\left\{\cos\left(\Theta_n^L(\theta)\right), \cos\left(\Theta_n^U(\theta)\right)\right\}\right], & \pi + 2i\pi \in \Theta_n^I, \end{cases} \tag{8a}$$

$$\sin\left(\Theta_n^I(\theta)\right) = \begin{cases} \left[\sin\left(\Theta_n^L(\theta)\right), \sin\left(\Theta_n^U(\theta)\right)\right], & \dfrac{\partial\sin\left(\Theta_n^I\right)}{\partial\Theta_n^I} > 0, \\ \left[\sin\left(\Theta_n^U(\theta)\right), \sin\left(\Theta_n^L(\theta)\right)\right], & \dfrac{\partial\sin\left(\Theta_n^I\right)}{\partial\Theta_n^I} < 0, \\ \left[\min\left\{\sin\left(\Theta_n^L(\theta)\right), \sin\left(\Theta_n^U(\theta)\right)\right\}, 1\right], & \dfrac{\pi}{2} + 2i\pi \in \Theta_n^I, \\ \left[-1, \max\left\{\sin\left(\Theta_n^L(\theta)\right), \sin\left(\Theta_n^U(\theta)\right)\right\}\right], & -\dfrac{\pi}{2} + 2i\pi \in \Theta_n^I. \end{cases} \tag{8b}$$

3. Array Synthesis in the Presence of Array Excitation Errors

For ideal array, array synthesis has been studied in many literatures. However, array errors bring bad influence on the performance of the designed array pattern, for example, decrease of array gain and increase of sidelobe level. To avoid these problems, a solution is to take array error into account when designing the array. In [14], particle swarm optimization (PSO) technique is combined with interval arithmetic to realize array synthesis in the presence of array excitation amplitude error. However, PSO suffers from high computational loads. In this paper, array excitation in the presence of array excitation amplitude and phase errors is optimized by convex programming which can decrease computational loads.

The interval of array power pattern considering excitation amplitude and excitation phase error can be expressed as

$$P_{\alpha,\varphi}^I(\theta) = \left|\sum_{n=0}^{N-1} \alpha_n^I e^{j\Theta_n^I(\theta)}\right|^2, \tag{9}$$

where $P_{\alpha,\varphi}^I(\theta) = [P_{\alpha,\varphi}^L(\theta), P_{\alpha,\varphi}^U(\theta)]$.

To optimize the array excitation, the following cost function is constructed:

$$\boldsymbol{\alpha}^{\text{opt}} = \arg\left\{\max_{\boldsymbol{\alpha}}\left[P_{\alpha,\varphi}^L(\theta_0)\right]\right\}, \tag{10a}$$

$$\text{subject to} \quad P_{\alpha,\varphi}^U(\theta_s)\Big|_{\boldsymbol{\alpha}=\boldsymbol{\alpha}_{\text{opt}}} \le M(\theta_s), \quad \theta_s \notin \Omega, \tag{10b}$$

where θ_0 denotes the look direction, Ω denotes the mainlobe region, and θ_s denotes the sidelobe region. The proposed cost function aims to maximize the lower bound of the array radiation pattern at the look direction and simultaneously guarantees that the upper bound of the array pattern in sidelobe region does not exceed a preset value.

Based on (4b), the objective function can be equivalently expressed as

$$\begin{aligned} P_{\alpha,\varphi}^L(\theta_0) &= \left(\sum_{n=0}^{N-1} \alpha_n^L \cos^L\left(\Theta_n(\theta_0)\right)\right)^2 \\ &\quad + \left(\sum_{n=0}^{N-1} \alpha_n^L \sin^L\left(\Theta_n(\theta_0)\right)\right)^2 \\ &= \left(\sum_{n=0}^{N-1} \alpha_n^L \cos\left(\Theta_n^U(\theta_0)\right)\right)^2 \\ &\quad + \left(\sum_{n=0}^{N-1} \alpha_n^L \sin\left(\Theta_n^L(\theta_0)\right)\right)^2 \\ &= \left(\sum_{n=0}^{N-1} (\alpha_n - \varepsilon_n) \cos\left(\Theta_n^U(\theta_0)\right)\right)^2 \\ &\quad + \left(\sum_{n=0}^{N-1} (\alpha_n - \varepsilon_n) \sin\left(\Theta_n^L(\theta_0)\right)\right)^2, \end{aligned} \tag{11}$$

where ε_n is the excitation amplitude error of the nth element.

Following (5a), (10b) can be expressed as

$$\begin{aligned} P_{\alpha,\varphi}^U(\theta_s) &= \left(\left|\sum_{n=0}^{N-1} \mu\left\{\alpha_n^I \cos\left(\Theta_n^I(\theta_s)\right)\right\}\right| \right. \\ &\quad \left. + \frac{1}{2}\sum_{n=0}^{N-1} \omega\left\{\alpha_n^I \cos\left(\Theta_n^I(\theta_s)\right)\right\}\right)^2 \\ &\quad + \left(\left|\sum_{n=0}^{N-1} \mu\left\{\alpha_n^I \sin\left(\Theta_n^I(\theta_s)\right)\right\}\right| \right. \\ &\quad \left. + \frac{1}{2}\sum_{n=0}^{N-1} \omega\left\{\alpha_n^I \sin\left(\Theta_n^I(\theta_s)\right)\right\}\right)^2 \le M(\theta_s). \end{aligned} \tag{12}$$

It is observed from (11) and (12) that $P_{\alpha,\varphi}^L(\theta_0)$ and $P_{\alpha,\varphi}^U(\theta_s)$ are quadratic functions with respect to α_n. Therefore, convex programming can be used to solve (10a) and (10b).

4. Computer Simulations

4.1. IA-Based Method. A uniform linear array (ULA) with $N = 10$ half-wavelength spaced sensors is considered. The nominal amplitudes α_n ($n = 0, 1, \ldots, N-1$) based on Chebyshev synthesis method are given in Table 1, which generates a power pattern with the sidelobe level −20 dB. The interval of the excitation amplitude and phase are assumed to be $\alpha_n^I = [\alpha_n - (\delta\alpha_n)\alpha_n, \alpha_n + (\delta\alpha_n)\alpha_n]$ and $\varphi_n^I = [\varphi_n - \delta\varphi_n, \varphi_n + \delta\varphi_n]$.

$Q = 5000$ array patterns $P(u)$, where $u = \sin\theta$, have been generated by randomly selecting the amplitude and phase from these intervals with uniform distribution. Figures 1–3 show all Q beams as well as the IA-computed power pattern bounds with different amplitude and phase intervals.

Table 1: Amplitude distribution ($N = 10$, $d = \lambda/2$; Chebyshev: $\mathrm{SLL}_{\mathrm{ref}} = -20$ dB).

$\alpha_0 = \alpha_9$	$\alpha_1 = \alpha_8$	$\alpha_2 = \alpha_7$	$\alpha_3 = \alpha_6$	$\alpha_4 = \alpha_5$
1.000	0.926	1.213	1.436	1.559

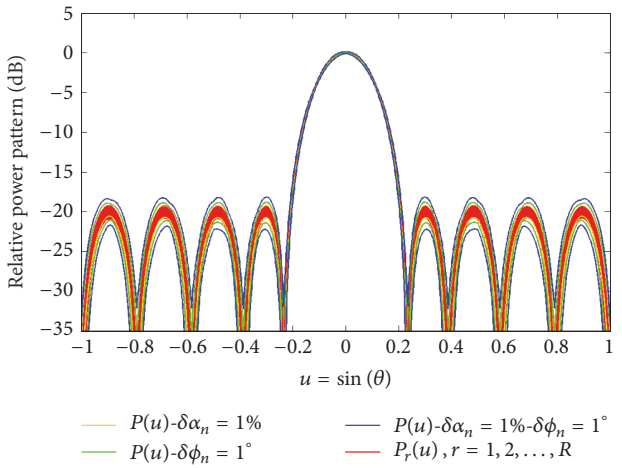

Figure 1: Bounds of the power pattern $P(u)$ based on IA with $\delta\alpha_n = 1\%$, $\delta\varphi_n = 1^\circ$.

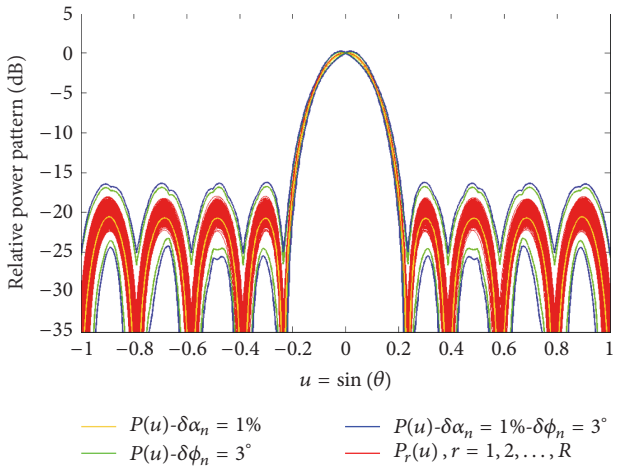

Figure 2: Bounds of the power pattern $P(u)$ based on IA with $\delta\alpha_n = 1\%$, $\delta\varphi_n = 3^\circ$.

It can be observed from the figures that the IA-based methods which consider the amplitude or phase error only are unable to consistently give correct bounds of the power pattern. For the proposed method, the bounds are correct for all situations.

For different expected sidelobe level ($\mathrm{ISLL}_{\mathrm{ref}}$), Figures 4–6 show the derived SLL interval, main-lobe bandwidth (BW) interval, and the directivity (D) interval with different amplitude and phase intervals, respectively.

It can be concluded from these figures that synthesis of the desired array pattern becomes difficult when the excitation errors are large, since higher excitation errors lead to larger interval width, for example, for $\mathrm{SLL}_{\mathrm{ref}} = -25$ dB,

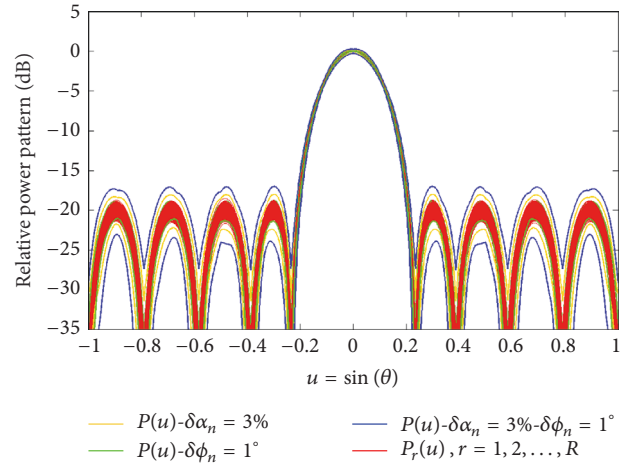

Figure 3: Bounds of the power pattern $P(u)$ based on IA with $\delta\alpha_n = 3\%$, $\delta\varphi_n = 1^\circ$.

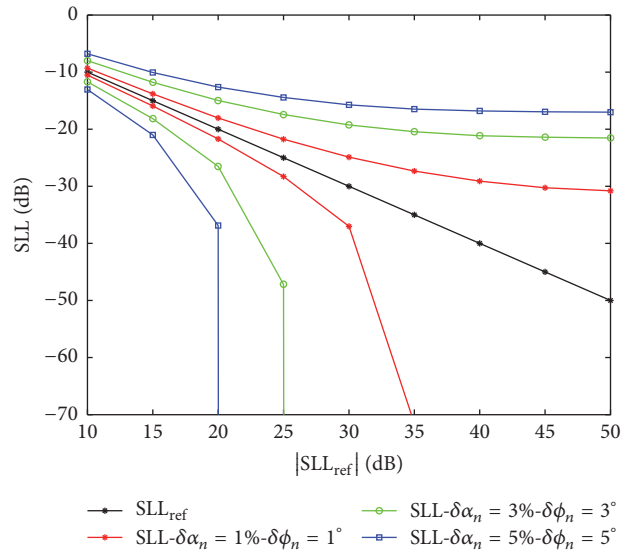

Figure 4: SLL interval based on IA against $\mathrm{ISLL}_{\mathrm{ref}}$.

$\omega\{\mathrm{SLL}\}|_{\delta\alpha_n=1\%,\delta\varphi_n=1^\circ} = 6.54$ dB, $\omega\{\mathrm{SLL}\}|_{\delta\alpha_n=3\%,\delta\varphi_n=3^\circ} = 29.75$ dB, and $\omega\{\mathrm{SLL}\}|_{\delta\alpha_n=5\%,\delta\varphi_n=5^\circ} = \infty$. From Figure 4, as $\mathrm{ISLL}_{\mathrm{ref}}$ increases, the upper bound of the SLL approaches a constant higher than the expected SLL, which means it is unguaranteed to achieve an array pattern with low sidelobe level in the presence of excitation error. Also, from the figure, the precision of the excitation to achieve relative satisfactory performance can be derived; for example, for $\mathrm{ISLL}_{\mathrm{ref}} = 20$ dB, $\delta\alpha_n = 1\%$, $\delta\varphi_n = 1^\circ$ guarantees that the derived SLL is within $[-21.71, -18.03]$ dB.

4.2. IA-CP Based Array Synthesis. In this simulation, array excitation amplitude and phase errors are taken into account. The interval of the excitation amplitude and phase are assumed to be $\alpha_n^I = [\alpha_n - (\delta\alpha_n)\alpha_n, \alpha_n + (\delta\alpha_n)\alpha_n]$ and $\varphi_n^I = [\varphi_n - \eta, \varphi_n + \eta]$. A ULA with 20 half-wavelength spaced elements is considered. The constraint of the sidelobe level $M(\theta_s)$ is set to

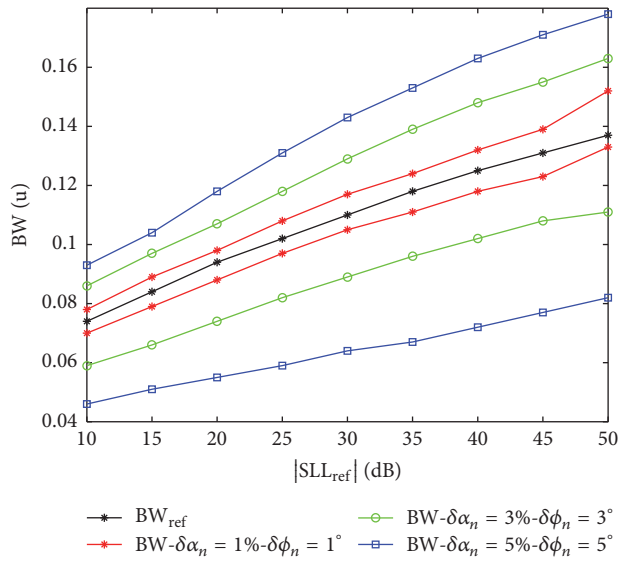

Figure 5: BW interval based on IA against $\mathrm{ISLL}_{\mathrm{ref}}$.

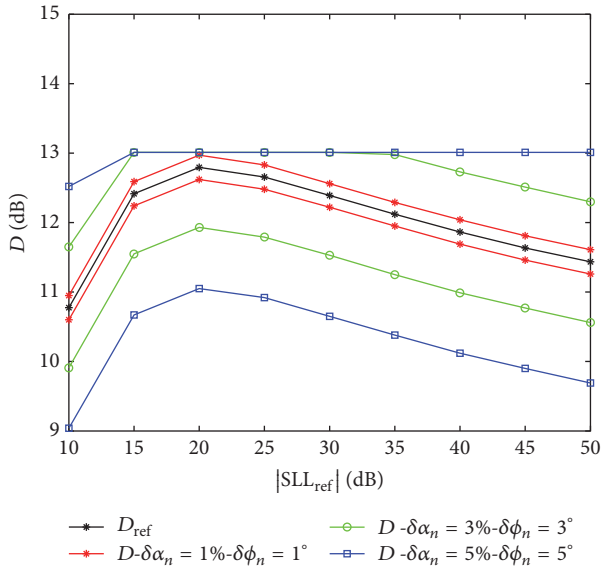

Figure 6: Directivity interval based on IA against $\mathrm{ISLL}_{\mathrm{ref}}$.

0 dB. Figure 7 shows the derived array excitation amplitudes with $\delta\alpha_n = 1\%$, $\eta = 1^\circ$ and $\delta\alpha_n = 3\%$, $\eta = 3^\circ$. Figures 8 and 9 show the generated array radiation patterns using the derived excitation amplitudes.

It can be observed from Figure 7 that when excitation errors become large, the derived array excitation amplitudes decrease. It is natural to see this since larger errors yield higher upper bound of array pattern. Therefore, in order to satisfy sidelobe constraint, excitation amplitudes become smaller. Figures 8 and 9 validate this conclusion. It can be observed from Figure 9 that the main-lobe gain with $\delta\alpha_n = 3\%$, $\eta = 3^\circ$ is smaller than that with $\delta\alpha_n = 1\%$, $\eta = 1^\circ$. For the two cases, the upper bounds of the radiation pattern in sidelobe region meet the constraint, that is, smaller than 0 dB.

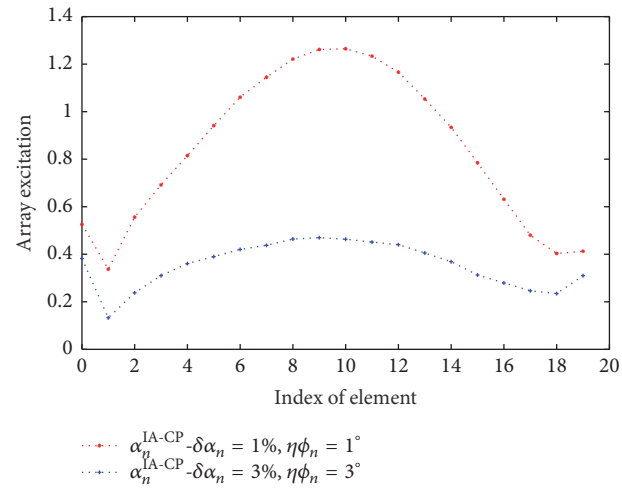

Figure 7: Optimized array excitation amplitudes using IA-CP method.

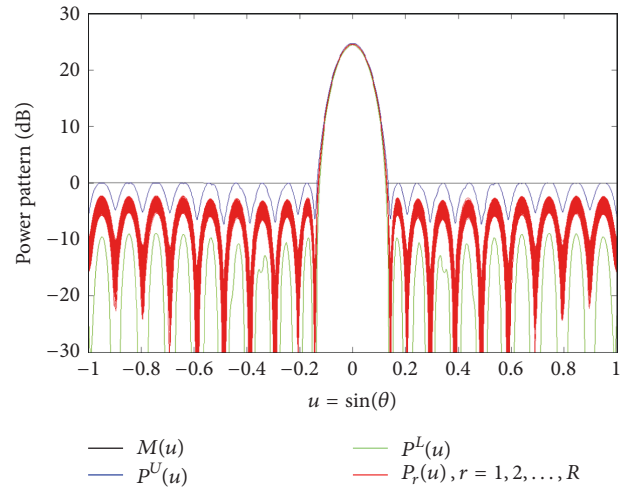

Figure 8: Array radiation patterns using the optimized array excitation ($\delta\alpha_n = 1\%$, $\eta = 1^\circ$).

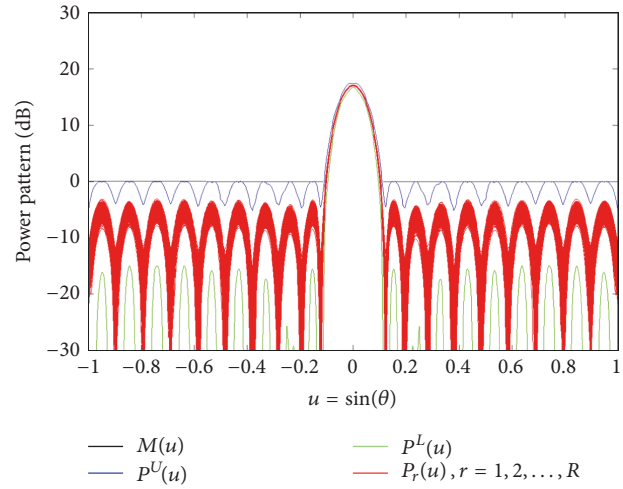

Figure 9: Array radiation patterns using the optimized array excitation ($\delta\alpha_n = 3\%$, $\eta = 3^\circ$).

5. Conclusion

In this paper, a novel approach based on interval analysis has been proposed to efficiently access the impact on power pattern when random manufacturing errors are present on both the array weights and the element position. The upper and lower bounds of the corresponding radiated array pattern are deduced according to the rules of the interval arithmetic. The obtained bounds can be used to facilitate array synthesis when array weights error and elements position error are considered in real applications. Simulation results demonstrate the robustness and reliability of the deduced new bounds. Furthermore, with the derived bounds, array synthesis is realized in the presence of excitation errors.

Conflicts of Interest

The authors declare that there are no conflicts of interest regarding the publication of this paper.

References

[1] C. A. Balanis, *Antenna Theory: Analysis and Design*, Wiley, New York, NY, USA, 3rd edition, 2005.

[2] J. Ruze, "The effect of aperture errors on the antenna radiation pattern," *Il Nuovo Cimento*, vol. 9, no. 3, pp. 364–380, 1952.

[3] J. K. Hsiao, "Design of error tolerance of a phased array," *Electronics Letters*, vol. 21, no. 19, pp. 834–836, 1985.

[4] P. Rocca, L. Manica, N. Anselmi, and A. Massa, "Analysis of the pattern tolerances in linear arrays with arbitrary amplitude errors," *IEEE Antennas and Wireless Propagation Letters*, vol. 12, pp. 639–642, 2013.

[5] N. Anselmi, L. Manica, P. Rocca, and A. Massa, "Tolerance analysis of antenna arrays through interval arithmetic," *Institute of Electrical and Electronics Engineers. Transactions on Antennas and Propagation*, vol. 61, no. 11, pp. 5496–5507, 2013.

[6] R. E. Moore, *Interval Analysis*, Prentice-Hall, Englewood Cliffs, NJ, USA, 1966.

[7] E. R. Hansen, "On solving systems of equations using interval arithmetic," *Mathematics of Computation*, vol. 22, pp. 374–384, 1968.

[8] A. Neumaier, "Interval iteration for zeros of systems of equations," *BIT Numerical Mathematics*, vol. 25, no. 1, pp. 256–273, 1985.

[9] E. Hansen, "Global optimization using interval analysis—the multidimensional case," *Numerische Mathematik*, vol. 34, no. 3, pp. 247–270, 1980.

[10] E. Hansen and G. W. Walster, *Global Optimization Using Interval Analysis*, vol. 264, CRC Press, New York, NY. USA, 2004.

[11] R. Boche, "Complex interval arithmetic with some applications Lockheed Missiles & Space Company," Tech. Rep. pp. 1-33, Sunnyvale, Calif, USA, 1966.

[12] R. S. Elliott, *Antenna Theory and Design IEEE Press*, Wiley, Hoboken, NJ, USA, 2nd edition, 2003.

[13] L. Poli, P. Rocca, N. Anselmi, and A. Massa, "Dealing with uncertainties on phase weighting of linear antenna arrays by means of interval-based tolerance analysis," *Institute of Electrical and Electronics Engineers. Transactions on Antennas and Propagation*, vol. 63, no. 7, pp. 3229–3234, 2015.

[14] L. Manica, N. Anselmi, and P. Rocca, "Robust mask-constrained linear array synthesis through an interval-based particle SWARM optimization," *IET Microwaves, Antennas & Propagation*, vol. 7, no. 12, pp. 976–984, 2013.